Waste and Biomass Valorization (2024) 15:5043–5052
https://doi.org/10.1007/s12649-024-02493-5

ORIGINAL PAPER

Characterization of Acid-Mechanical Milling Pretreated Rice Straw for Subcritical Water Hydrolysis

Wei Yang[1,2,3] · Fan Yang[2] · Shengji Wu[2] · Lei Che[2,3]

Received: 26 November 2023 / Accepted: 11 March 2024 / Published online: 18 April 2024

Abstract

Ball milling of rice straw impregnated with sulfuric acid (RS-S), hydrochloric acid (RS-H), acetic acid (RS-A), or nitric acid (RS-N) were carried out in this study. Physicochemical analysis and subcritical water hydrolysis were performed to evaluate the effect of acid species on ball milling treatment of rice straw. Acetic acid and solo ball milling treatment showed little effect on solubility, thermal stability and crystalline structure of rice straw, while hydrochloric acid, acetic acid and nitric acid significantly improved the solubility and decreased the crystallinity index and thermal stability of rice straw. Sulfuric acid was found to be the most efficient acid to destroy the rice straw structure during ball milling followed by nitric acid and hydrochloric acid, attributed to its long retention on rice straw surface after drying. The effective cleavage of holocellulose-lignin chemical linkages in RS-S during pretreatment made the hydrolysis products of RS-S easier to be hydrolyzed to biochar at high reaction temperatures, resulting in the increased solid residue yield. The breakage of crystallites and holocellulose-lignin chemical linkages greatly improved the reactivity of RS-S, resulting in the lower temperature and activation energy required to initiate the hydrolysis reaction compared with those of rice straw and RS-A.

Statement of novelty

Biomass is a promising platform for both bioenergy and feed stock chemicals. However, the rigid structure of biomass made it difficult to be hydrolyzed and converted to biofuels and value-added chemicals in subcritical water. Acid/alkaline pretreatment, a broadly employed biomass pretreatment method could efficiently cleave the chemical bonds in biomass. However, it suffers equipment corrosion and environmental pollution because of the high concentration of acid/alkaline used. In this study, diluted acids (H_2SO_4, HCl, CH_3COOH and HNO_3) were employed to impregnate rice straw, followed by ball milling, in order to improve the accessibility of rice straw during hydrolysis in subcritical water. H_2SO_4 was found to be the most efficient acid to destroy the rice straw structure during ball milling, which resulted in the lower activation energy needed to initiate the hydrolysis reaction in subcritical water, and higher contents of value-added chemicals in the hydrolysate.

Highlights

- H_2SO_4 was the most efficient acid to destroy the RS structure during ball milling.
- Acid-associated mechanical treatment can cleave the glycosidic bonds in RS.
- The solubility of RS was greatly improved after acid impregnation and ball milling.
- The destruction of hydrogen and glycosidic bonds made RS easier to be hydrolyzed.

✉ Fan Yang
02567@zjhu.edu.cn

✉ Shengji Wu
wu_shengji@hotmail.com

[1] School of Environmental Science and Engineering, Tianjin University, Tianjin 300072,, China

[2] College of Engineering, Huzhou University, No. 759, East 2nd Road, Huzhou 313000, China

[3] Zhejiang ECO Environmental Technology Co., Ltd, No. 1188, Wuxing District, Huzhou 313000, China

Graphical Abstract

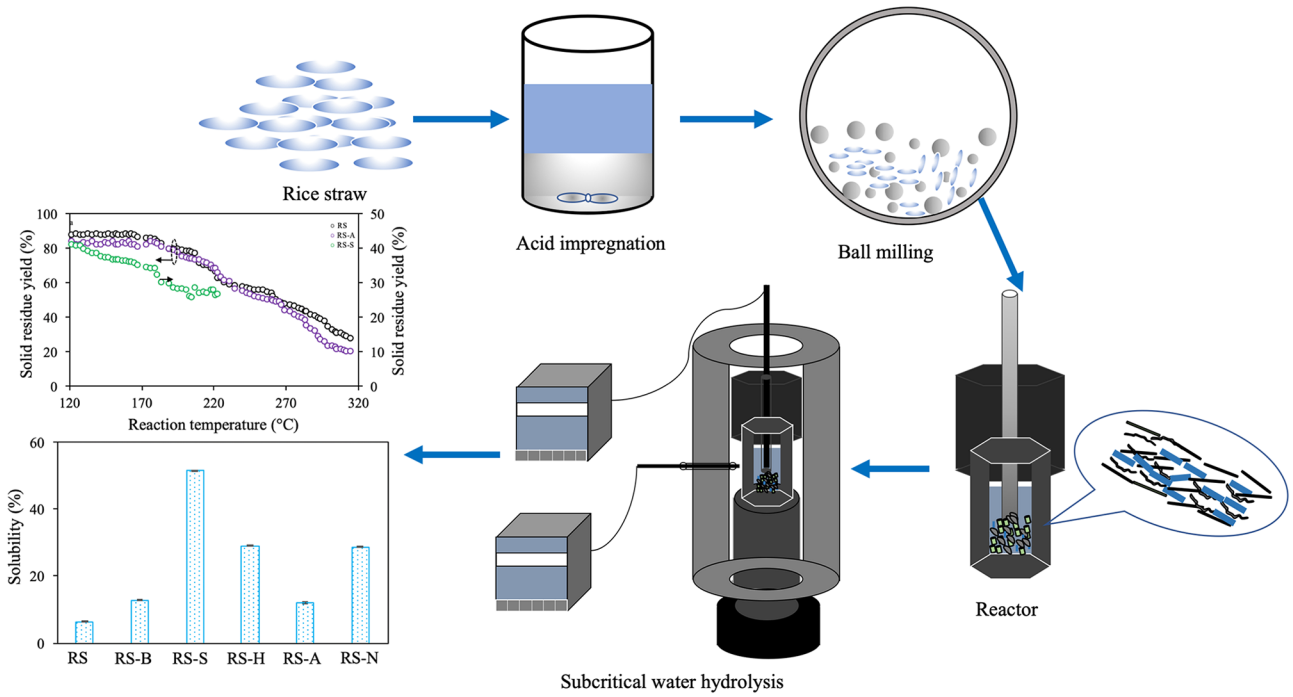

Keywords Acid-mechanical milling pretreatment · Acid species · Rice straw · Subcritical water · Hydrolysis kinetics

Introduction

Biomass, the most abundant renewable resource in the world is considered to be a promising candidate to replace fossil-derived fuels and chemicals [1]. Various technologies such as subcritical water treatment have been employed to convert biomass to biofuels and value-added chemicals [2, 3]. However, the rigid structure caused by cellulose crystallinity and the matrix formed by lignin and hemicellulose reduce the conversion efficiency of biomass to value-added chemicals in subcritical water [4, 5]. In order to address the above hurdle, various pretreatment methods such as ionic liquid, deep eutectic solvent, mechanical milling and acidic/alkaline pretreatment were thus tested to improve the reactivity of biomass [6, 7].

Among all the pretreatment method, acid/alkaline pretreatment had been broadly employed to treat raw biomass for reactive substrates production, owing to its high efficiency to cleave the chemical bonds such as glucosidic bonds and α-ether bonds between hemicellulose and lignin in biomass [1, 8]. However, high concentration of acid/alkaline is always needed in order to efficiently hydrolyze biomass, which will cause equipment corrosion and environmental pollution [8]. What is more, the acid/alkaline chemical agents that anchor onto the biomass framework during pretreatment are hard to wash off and high cost was thus required to recover the spent chemicals [8, 9].

Pretreatment of biomass with mechanical milling has attracted much attention in recent years, because it could induce different extents of size reduction and various mechanochemical effects [10]. After mechanical milling, surface area and solubility of biomass can be significantly improved, while crystallinity degree, particle size and thermal stability are reduced [11–13]. Nevertheless, a large amount of energy and a long time are always required, to break down the biomass structure and reduce the biomass particle size [14]. In addition, the molecular mass of biomass components could be only marginally decreased by solo ball milling treatment. Combination of diluted acid impregnation and mechanical milling could largely improve the milling efficiency and reduce the cost for biomass pretreatment [15]. The cellulose in biomass could be effectively depolymerized and decrystallized after mechanical milling, due to the acid-catalyzed conversion of cellulose to glucan oligomers with α-(1→6) glycosidically linked branches [16, 17]. The acidulated biomass after mechanical milling could be efficiently converted to valuable chemicals by means of catalytic hydrolysis in subcritical water [18–21]. However, to the best of our knowledge, very little is known about hydrolysis behavior of pretreated biomass under subcritical water conditions, which will affect the optimum conditions for effective

hydrolysis of biomass to value-added chemicals. Besides, the effect of impregnation using different acids on biomass structure can be diverse, which will significant influence the hydrolysis mechanism of biomass. In this study, rice straw (RS) that applied as a model of biomass sample was pretreated by acid impregnation (H_2SO_4, HCl, CH_3COOH and HNO_3) and ball milling. The effect of acid species on physicochemical properties, hydrolysis behavior as well as hydrolysis kinetics of pretreated RS was investigated to determine the optimum conditions for RS hydrolysis in subcritical water.

Experimental Details

Materials

RS collected from Huzhou city, Zhejiang Province was selected as raw biomass. The RS was dried, crushed and sieved to select the particles with a diameter of < 0.3 mm, before experiment. The cellulose content, hemicellulose content and lignin content in the RS were analyzed to be 30.2%, 24.6% and 14.8%, respectively. H_2SO_4, HCl and HNO_3 were received from Hangzhou Shuanglin Chemical Industry Co., Ltd. (Zhejiang, China). Reagents of 3,5-dinitrosalicylic acid, sodium potassium tartrate, phenol, glucose, ascorbic acid, ethanol and acetic acid were received from Shanghai Aladdin Industrial Co., Ltd.

Rice Straw Pretreatment

15 g of RS and 30 mL of diluted acid (H_2SO_4, HCl, CH_3COOH and HNO_3) were charged into a glass container. The slurry was then mixed and oven-dried to prepare the acidulated RS. The oven-dried RS was then ball-milled for 4 h at 300 r min^{-1} by a planetary ball milling machine. The samples pretreated with H_2SO_4, HCl, CH_3COOH and HNO_3 as well as ball milling were defined as RS-S, RS-H, RS-A and RS-N, respectively. The RS only pretreated with ball milling was named as RS-B.

Hydrolysis of Rice Straw in Subcritical Water

RS, RS-B, RS-S, RS-H, RS-A and RS-N were hydrolyzed at 180, 200, 220, 240 and 260 °C for 5 min, in a batch reactor (10 mL) made by SUS316 stainless steel. At the end of hydrolysis, vacuum filtration was applied to separate the hydrolysate and solid residue in the reactant, which were then stored at 4 °C and oven-dried, respectively.

Hydrolysis behaviors of RS, RS-A and RS-S were investigated in the same reactor. For each run, the reactor loaded with 7 mL distilled water and 150 mg of sample was immersed into a preheated ceramic furnace (500 °C) controlled by a single-display proportional-integral-derivative controller. The reaction temperature started at 100 °C, and heated to the desired temperature at a heating rate of 18 °C min^{-1}. The reactor was treated at various reaction times according to the hydrolysis behavior of sample. The reactor was cooled down immediately by immersing into an ice bath to fully stop the reaction when the reactor reached the desired temperature. The hydrolysate and solid residue were also separated through vacuum filtration.

A model-fitting method, Coats-Redfern method, was applied to estimate the hydrolysis kinetics and kinetic parameters of RS, RS-A and RS-S in subcritical water, according to previous research [5]. The expression of reaction models functions in Coats-Redfern method is listed on Table S1.

Characterization

FTIR (Nicolet iS20, Thermo Scientific, MA, USA) and XRD (D8 Advance, Bruker, Germany) tests were performed to study the functional group and structure change of RS with and without pretreatment, respectively. Solubility was evaluated through dissolving 1 g of RS with and without pretreatment into 20 mL of deionized water. Total carbohydrate content (TCH) in the hydrolysate was determined by a phenol-sulfuric acid method with some modification. Reducing sugar content (RDS) was evaluated by a modified dinitrosalicylic colorimetric method and free radical scavenging activity (FRSA) was analyzed by a modified 1,1-diphenyl-a-picrylhydrazyl hydrate method. The detail description of above analytic methods was provided in our previous research [5].

Results and Discussion

Properties of Rice Straw after Pretreatment

Various mechanochemical effects would be initiated during acid and ball-milling pretreatment of RS, resulting in the obvious change of RS structure. The FTIR spectra of RS with and without pretreatment are presented in Fig. 1. The band at 3400 cm^{-1} was indicative of O-H stretching band, which was caused by the vibration of hydrogen bonded hydroxyl group [12, 22]. The bands presented at 1100 and 1040 cm^{-1} are relevant to C-O vibration of crystalline cellulose and C-O stretching of cellulose, respectively. The peak intensities of above peaks became more intense after pretreatment, which ascribed to the formation of glucan through repolymerization of cellulose derived oligomers [23]. The intensities of other bands, such as aliphatic C-H stretching

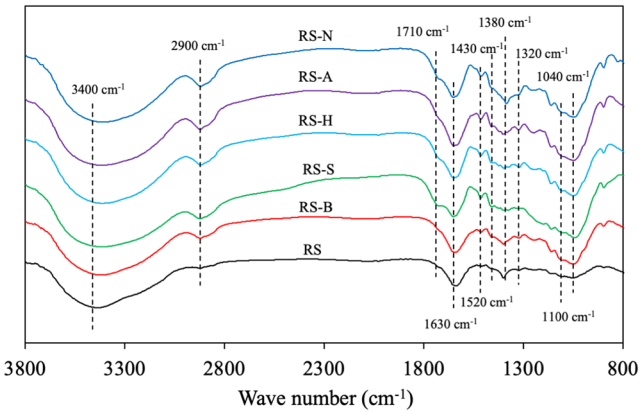

Fig. 1 FTIR spectra of RS, RS-B, RS-S, RS-H, RS-A and RS-N

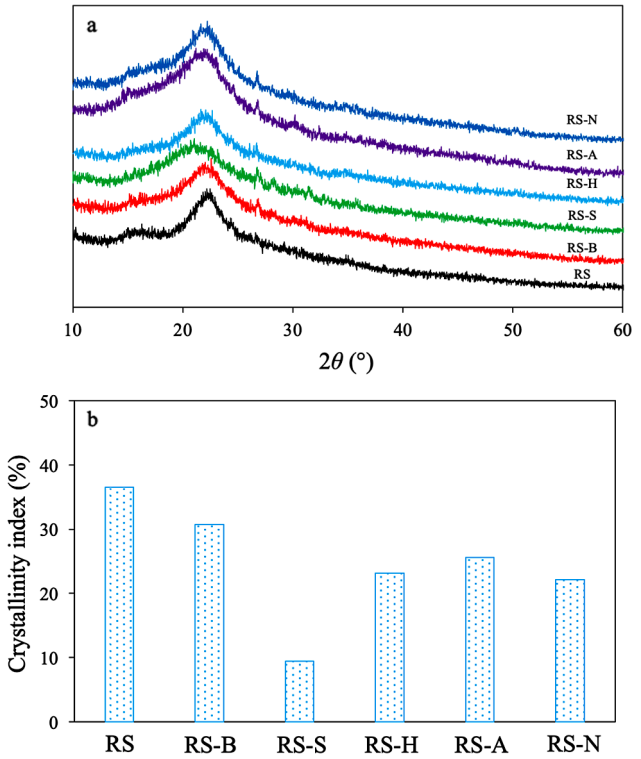

Fig. 2 (**a**) XRD patterns and (**b**) crystallinity index of RS, RS-B, RS-S, RS-H, RS-A and RS-N

band at 2900 cm^{-1}, C = O stretching band at 1710 cm^{-1} and C-H deformation band at 1380 cm^{-1} also increased after pretreatment. The lignin-related peaks corresponded to aromatic skeletal vibration (1630 and 1520 cm^{-1}), C-H bending (1430 cm^{-1}) and syringyl (S) and guaiacyl (G) units (1320 cm^{-1}) existed in all samples, which implied that the lignin structure in RS was not destroyed during pretreatment.

Figure 2 shows the XRD diffraction spectra of RS, RS-B, RS-S, RS-H, RS-A and RS-N. A weak peak and a sharp peak presented at 2θ values around 14.8° and 22°, respectively, in all samples, which are the characteristic of typical forms of

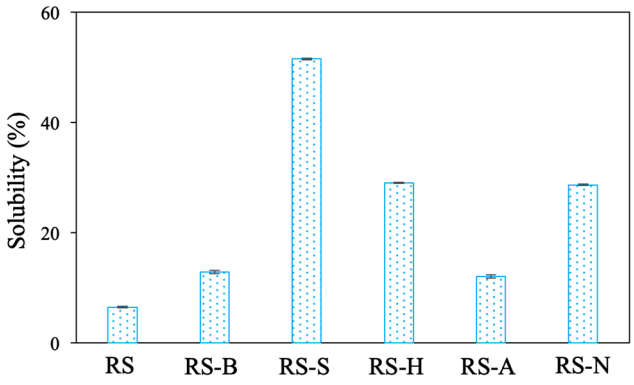

Fig. 3 Solubility of RS, RS-B, RS-S, RS-H, RS-A and RS-N ($n = 3$)

cellulose I (Fig. 2a). The presence of above peaks indicated that the crystal structure of cellulose in RS still remained after pretreatment. However, diffraction peak at 2θ = 22° that corresponded to crystal face of (002) became weaker after pretreatment. Meanwhile, crystallinity index of RS, which was calculated by the peak height method decreased after acid and ball milling pretreatment [24], as shown in Fig. 2b. The above phenomena indicated the breakage of crystallites in cellulose, which occurred through destruction of inter and intra hydrogen bonds as well as glycosidic bonds in RS during pretreatment. RS-S showed the weakest crystalline peak intensity and the lowest crystallinity index among all the samples, which implied that H_2SO_4 was the most effective acid to destroy the crystalline structure of cellulose in rice straw. The loss of cellulose crystal structure through ball milling would result in changes in the atomic spacing. For example, transition of C6 group to a different conformation or different rotational angles about the β-(1→4) glycosidic linkage might increase or decrease spacings between atoms located in adjacent glucose molecules, which led to the shift of crystalline peak [25]. The reduction of long-range forces in the smaller crystallinities of cellulose would lead to the shift of crystalline peak to lower 2θ value [26]. In the present study, the pretreated samples showed lower 2θ values of crystalline peak compared with that of RS, indicating the increase of spacing between atoms located in adjacent glucose molecules and/or reduction of long-range forces in the smaller crystallinities of cellulose (Fig. 2a). The lowest 2θ value of crystalline peak in RS-S further confirmed the efficiency of H_2SO_4 to destroy the crystalline structure of cellulose in rice straw.

The breakage of hydrogen bond and glycosidic bond in RS would significantly affect its solubility. Figure 3 shows the solubility of RS, RS-B, RS-S, RS-H, RS-A and RS-N. We could observe that RS (6.5%) was sparingly soluble in water. Solo ball milling as well as CH_3COOH impregnation and ball milling treatment showed low efficiency on elevating the solubility of RS. However, the solubility of

RS was greatly elevated after strong acid (H_2SO_4, HCl and HNO_3) impregnation and ball milling treatment. Figure S1 presents the TCH content, RDS content and FRSA in the extracts from RS, RS-B, RS-S, RS-H, RS-A and RS-N. The extracts of RS and RS-B presented lower TCH and RDS contents than those of RS-B, RS-S, RS-H, RS-A and RS-N (Figs. S1a and S1b). This result indicated that the acid especially strong acid could accelerate the dissociation of RS on glycisidic bonds for saccharides release and solubility improvement during pretreatment. The FRSA in the extracts of RS-S, RS-H, RS-N and RS-A also increased, ascribed to the generation of new antioxidant compounds by depolymerization of holocellulose (Fig. S1c).

Compared with RS, RS-B, RS-H, RS-A and RS-N, RS-S showed the lowest crystallinity index, the highest solubility, TCH and RDS contents among all samples, indicating that H_2SO_4 was the most efficient acid to pretreat RS. This was ascribed to the lower volatile of H_2SO_4, which resulted in the more amount of H_2SO_4 remained on RS surface after drying. The remained H_2SO_4 on RS could act as an acid catalyst to improve the mechanical milling efficiency for glycisidic bonds destruction, leading to the lower crystallinity index compared with those pretreated with other acids. The dissociation energies required for glycisidic bonds destruction were supplied by the impact between ball and RS. It could also result in the formation of branched cello-oligomers with α-(1→6) linkages to significantly improve the solubility of RS-S [17, 27]. In addition, the acid catalyst could not be destroyed during mechanical milling, which enabled the further hydrolysis of RS-S to valuable chemicals in subcritical water.

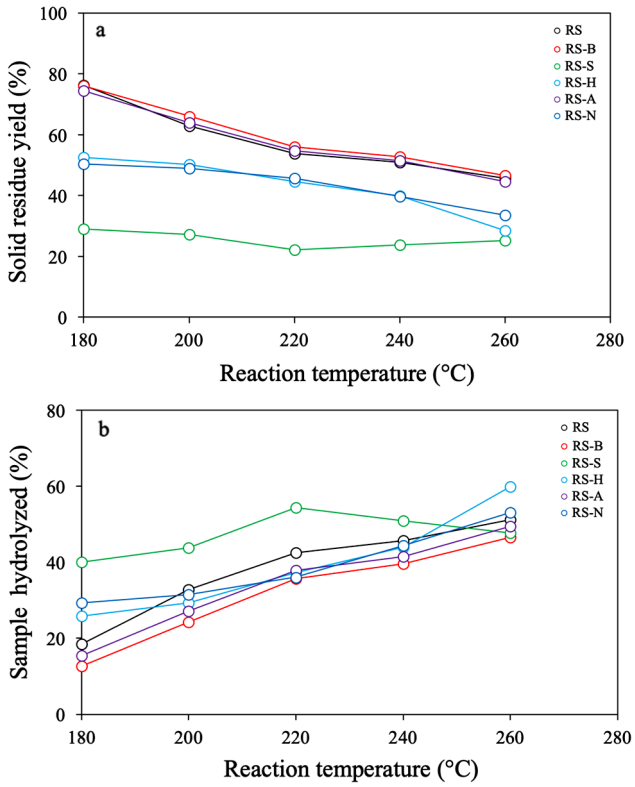

Fig. 4 (**a**) Solid residue yields of RS, RS-B, RS-S, RS-H, RS-A and RS-N, and (**b**) exact amount of sample hydrolyzed in RS, RS-B, RS-S, RS-H, RS-A and RS-N at the reaction temperatures of 180 to 260 °C ($n = 3$)

Thermal Stability of Rice Straw after Pretreatment

The thermal stability of RS with and without pretreatment was examined at 180 to 260 °C in subcritical water. As shown in Fig. 4a, the solid residue yield of RS decreased as the reaction temperature increased, which equaled 76.3%-45.6%. Solo ball milling as well as CH_3COOH impregnation and ball milling showed little effect on solid residue yield; the solid residue yields of RS-B and RS-A at 260 °C, following these pretreatment, were nearly the same to that of RS. The RS-S, RS-H and RS-N showed extremely low solid residue yields with the values of 29%, 52.5% and 50.4%, respectively, even at 180 °C. It seemed that the thermal stability of RS could be significantly reduced through strong acid impregnation and ball milling treatment. However, it worth noting that the solubility of RS significantly improved after pretreatment. The exact amount of sample hydrolyzed during subcritical water treatment was thus calculated in order to evaluate the thermal stability. We could clearly observe that the RS-S and RS-H presented lower thermal stability than that of RS, while the thermal stability of RS-B, RS-A and RS-N was similar to that of RS (Fig. 4b,). The decreased thermal stability was mainly caused by the breakage of crystallites in RS during pretreatment, as suggested by XRD measurement.

Characterization of Hydrolysate

The TCH, RDS and antioxidant compound contents in the hydrolysates obtained from RS, RS-B, RS-S, RS-H, RS-A and RS-N under various conditions are presented in Fig. 5. The reaction temperature presented significant effect on the TCH content and the maximum value of TCH content in the hydrolysate of RS obtained at 220 °C (Fig. 5a). The highest TCH contents in the hydrolysates of RS-B and RS-A were also obtained at 220 °C, whereas RS-S, RS-H and RS-N showed lower reaction temperature with the highest TCH content. The change tendencies of RDS contents in the hydrolysates of RS, RS-B and RS-A were similar to those of TCH content. Maximum RDS contents in the hydrolysates of RS, RS-B and RS-A were also obtained at 220 °C (Fig. 5b). In contrast, the reaction temperature for the highest RDS contents presented at 200 °C during hydrolysis of RS-S, RS-H and RS-N. The TCH and RDS contents in

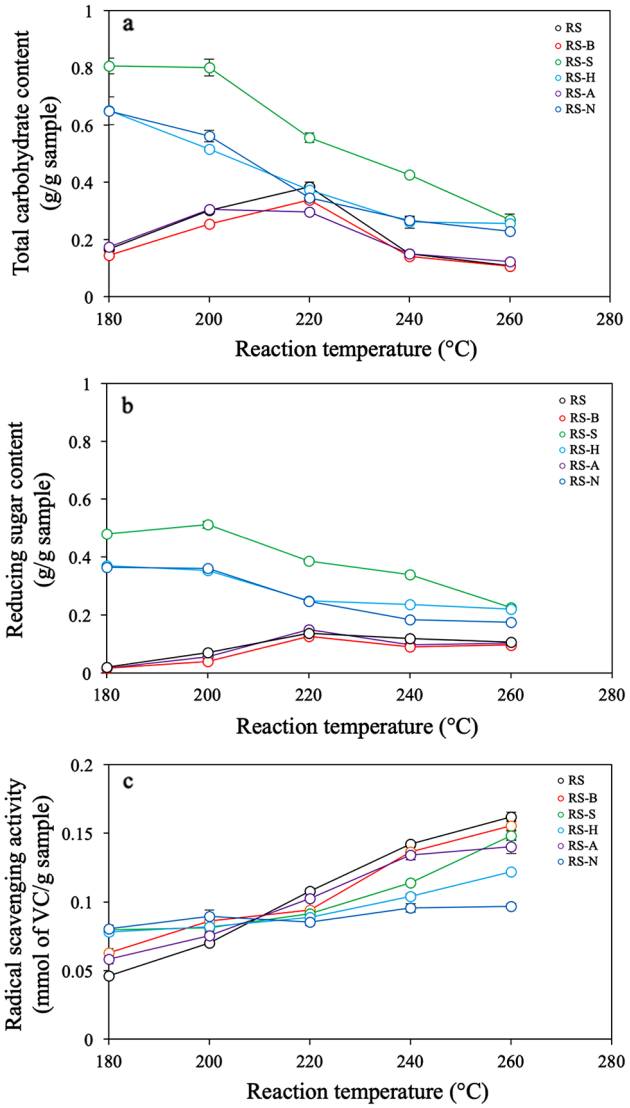

Fig. 5 (**a**) Total carbohydrate content, (**b**) reducing sugar content and (**c**) free radical scavenging activity in the hydrolysates of RS, RS-B, RS-S, RS-H, RS-A and RS-N ($n = 3$)

the hydrolysates of RS-S, RS-H and RS-N were obviously higher than those of RS, RS-B and RS-A under the same conditions. It was reported that the nature recalcitrance of cellulose arose by orderly intro- and intermolecular hydrogen bonds would prevent the interaction between their β-1,4-glycosidic bonds with external chemical reagents, which was intractable for monosaccharide release [28]. Therefore, the higher TCH and RDS contents in the hydrolysates of RS-S, RS-H and RS-N were due to the cleavage of glycosidic and hydrogen bonds, and breakage of crystallites in RS during pretreatment, making subcritical water easier to react with them. Besides, the acid remained on RS-S, RS-H and RS-N surfaces could facilitate the hydrolysis of holocellulose for saccharides production. The FRSA increased as the reaction temperature elevated from 180 to

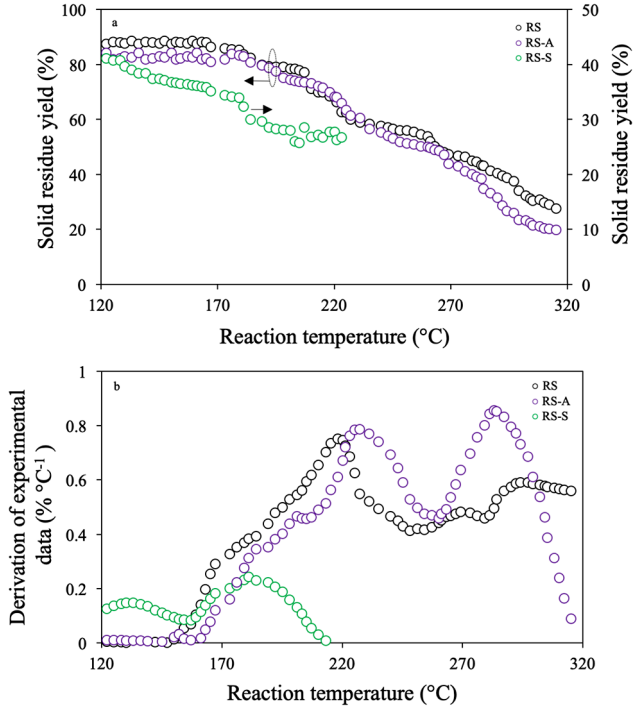

Fig. 6 (**a**) Hydrolysis behaviors and (**b**) derivation of experimental data of RS, RS-A and RS-S in subcritical water ($n = 3$)

260 °C for all samples, which indicated the improvement of extraction efficiencies for antioxidant compounds and formation of new antioxidant compounds [29]. The order of FRSA was determined to be RS > RS-B > RS-S > RS-H > RS-A > RS-N.

Hydrolysis Behaviors of Rice Straw, RS-A and RS-S

The hydrolysis behaviors of RS, RS-A and RS-S in subcritical water are presented on Fig. 6a. RS started its hydrolysis at 163 °C and the weight loss mainly occurred at 163–315 °C. The solid residue yield accounted for 27.7% of the weight of the original RS after hydrolysis. The entire hydrolysis period of RS could be divided into three sections, which presented at temperature ranges of 163–251 °C (Section I), 251–279 °C (Section II) and 279–315 °C (Section III). Three peaks, with mass loss rates of 0.75, 0.48 and 0.59% $°C^{-1}$, existed at 218, 269 and 294 °C, respectively (Fig. 6b). The weight losses of RS were mainly ascribed to the decomposition of cellulose, hemicellulose and a portion of lignin in section I and section III, while it was induced by the rapid hydrolysis of cellulose and hemicellulose in section II, according to previous research [29]. The RS-A showed a hydrolysis region of 176–315 °C. Three hydrolysis sections were also found in the entire hydrolysis region of RS-A at 176–205 °C (Section I), 205–260 °C (Section II) and 260–315 °C (Section III). The maximum weight loss rates in section I, section II and section III were determined to be 0.47 (201 °C), 0.78

(227 °C) and 0.86%°C^{-1} (283 °C), respectively. In contrast, the RS-S showed a much lower hydrolysis temperature with the value of 117 °C, indicating the significant reduction of thermal stability after pretreatment. The solid residue yield of RS-S reduced with increasing reaction temperature and fell to the lowest yield of 25.8% at 205 °C; but it showed an increase at higher reaction temperatures. The lower hydrolysis temperature of RS-S could be ascribed to the breakage of crystallites as suggested by XRD measurement, which made cellulose easier to be hydrolyzed in subcritical water. It was reported that some of the hydrolysis products derived from holocellulose could be further converted to biochar at high reaction temperature, resulting in the increased biochar yield [30, 31]. However, the formation of biochar would be inhibited if the holocellulose-lignin chemical linkages in biomass were not destroyed [30]. In this study, glucan was formed through repolymerization of cellulose derived oligomers during ball milling of H_2SO_4 impregnated RS, which could be easily dissolved and be hydrolyzed to valuable chemicals such as saccharides, furan derivatives and phenolic derivatives in subcritical water. Therefore, it was considered that the increase of solid residue yield of RS-S was due to the formation of large amounts of reactable products as well as breakage of holocellulose-lignin chemical linkages. Only two sections were found during hydrolysis of RS-S at reaction temperatures of 117–157 °C (Section I) and 157–205 °C (Section II), whose maximum weight loss rates were determined to be 0.15 (130 °C) and 0.24% °C^{-1} (181 °C), respectively.

Hydrolysis Kinetics of Rice Straw, RS-A and RS-S

Table 1 presents the activation energy (E), correlation coefficient (r^2) and pre-exponential factor (A_1) of RS for three sections, which calculated from the plotting results of experimental data (Fig. 6a) shown on Fig. S2. According to the correlation coefficients of kinetic models, it seemed that all the kinetic models agreed well to the experimental date of RS. However, the value of activation energy in section III (419.5 kJ mol^{-1}) calculated by the third-order kinetic model (F3) was so high that even radical reactions, which always occurred in near- and supercritical conditions could be triggered [32, 33]. Therefore, it was concluded that F3 kinetic model was not appreciate to explain the hydrolysis kinetics of RS. Activation energy that implies the lowest energy requirement for starting a reaction was one of the most important factors in controlling the hydrolysis process of RS. In other words, the higher value of activation energy, the more difficulty of a reaction starting. The one-way transport kinetic model (D1) in the diffusion models showed lower activation energy than those of two-way transport kinetic model (D2), three-way transport kinetic model (D3) and Ginstling-Brounshtein (D4), indicating the control of hydrolysis mechanism. As for the geometrical contraction and reaction-order models, they were controlled by the contracting model (R2) and the first-order kinetic model (F1), respectively. The average activation energies of RS were calculated to be 124.1, 55 and 93.7 kJ mol^{-1} in section I, section II and section III, respectively. The pre-exponential factors of RS were in the range of 3.0×10^{4}-1.9×10^{13} min^{-1}, 9.0×10^{-2}-7.4×10^{3} min^{-1} and 2.2×10^{0}-1.4×10^{19} min^{-1}, in section I, section II and section III, respectively.

Table 2 lists the hydrolysis kinetic parameters of RS-A. Diffusion models as well as F3 kinetic model in reaction-order models were not appropriate for expressing the hydrolysis mechanism of RS-A, because radical reactions could be hardly occurred at low reaction temperatures. In addition, covalent linkages always exist between holocellulose and lignin in biomass, the bond-dissociation energies of which depend on the covalent bond type (-390 to -100 kJ mol^{-1}) [34, 35]. If the hydrolysis kinetics of RS-A obeyed the above kinetic models, nearly all the above covalent

Table 1 Kinetic parameters of RS calculated by coats-redfern method

Model	Section I			Section II			Section III		
	E (kJ mol^{-1})	A_1 (min^{-1})	r^2	E (kJ mol^{-1})	A_1 (min^{-1})	r^2	E (kJ mol^{-1})	A_1 (min^{-1})	r^2
Diffusion models									
One-way transport (D1)	157.6	6.8×10^{12}	0.83	51.8	1.6×10^{1}	0.87	47.3	4.9×10^{0}	0.97
Two-way transport (D2)	163.2	1.6×10^{13}	0.84	63.3	5.2×10^{3}	0.88	73.4	1.5×10^{3}	0.98
Three-way transport (D3)	169.3	1.9×10^{13}	0.85	77.9	1.7×10^{3}	0.89	122.3	3.2×10^{7}	0.97
Ginstling-Brounshtein (D4)	165.2	6.1×10^{12}	0.84	68.1	1.3×10^{2}	0.88	88.6	1.3×10^{4}	0.97
Geometrical contraction models									
Contracting model (R2)	79.1	3.0×10^{4}	0.83	30.9	9.0×10^{-2}	0.85	44.3	2.2×10^{0}	0.97
Contracting volume (R3)	80.7	3.0×10^{4}	0.84	34.5	1.6×10^{-1}	0.86	56.4	2.7×10^{1}	0.97
Reaction-order models									
First-order (F1)	83.8	2.2×10^{5}	0.85	42.3	4.0×10^{0}	0.87	87.9	1.2×10^{5}	0.96
Second-order (F2)	93.9	3.7×10^{6}	0.88	71.2	7.4×10^{3}	0.9	229.7	1.4×10^{19}	0.93
Third-order (F3)	105.1	8.2×10^{7}	0.91	107.3	6.7×10^{7}	0.91	419.5	3.2×10^{37}	0.92

Table 2 Kinetic parameters of RS-A calculated by coats-redfern method

Model	Section I			Section II			Section III		
	E (kJ mol^{-1})	A_1 (min^{-1})	r^2	E (kJ mol^{-1})	A_1 (min^{-1})	r^2	E (kJ mol^{-1})	A_1 (min^{-1})	r^2
Diffusion models									
One-way transport (D1)	406.9	8×10^{40}	0.86	101.9	3.4×10^{6}	0.93	60	9.7×10^{1}	0.97
Two-way transport (D2)	410.8	1.2×10^{41}	0.87	109.8	1.4×10^{7}	0.94	84.4	2.0×10^{4}	0.98
Three-way transport (D3)	414.9	7.6×10^{40}	0.87	118.5	3.1×10^{7}	0.94	128.9	1.7×10^{8}	0.98
Ginstling-Brounshtein (D4)	412.2	3.7×10^{40}	0.87	112.7	6.5×10^{6}	0.94	98.2	1.2×10^{5}	0.99
Geometrical contraction models									
Contracting model (R2)	202.3	3.7×10^{18}	0.86	52.9	2.5×10^{1}	0.93	48.7	6.5×10^{0}	0.98
Contracting volume (R3)	203.6	3.2×10^{18}	0.86	55.1	3.0×10^{1}	0.94	59.8	6.6×10^{1}	0.98
Reaction-order models									
First-order (F1)	205.6	1.7×10^{19}	0.86	59.6	3.1×10^{2}	0.94	88.1	1.8×10^{5}	0.96
Second-order (F2)	211.8	8.9×10^{19}	0.86	74.5	1.7×10^{4}	0.96	222	4.9×10^{18}	0.87
Third-order (F3)	218.1	5.0×10^{20}	0.88	91.4	1.5×10^{6}	0.97	397.1	9.2×10^{35}	0.84

Table 3 Kinetic parameters of RS-S calculated by coats-redfern method

Model	Section I			Section II		
	E (kJ mol^{-1})	A_1 (min^{-1})	r^2	E (kJ mol^{-1})	A_1 (min^{-1})	r^2
Diffusion models						
One-way transport (D1)	126.4	9.0×10^{11}	0.91	69.8	2.9×10^{4}	0.96
Two-way transport (D2)	131.5	2.3×10^{12}	0.91	86.5	2.0×10^{6}	0.96
Three-way transport (D3)	136.9	2.8×10^{12}	0.92	111.1	5.9×10^{8}	0.94
Ginstling-Brounshtein (D4)	133.3	8.9×10^{11}	0.91	94.4	4.6×10^{6}	0.94
Geometrical contraction models						
Contracting model (R2)	63.7	1.2×10^{4}	0.9	45.7	3.4×10^{1}	0.93
Contracting volume (R3)	65.1	1.2×10^{4}	0.91	51.8	1.4×10^{2}	0.94
Reaction-order models						
First-order (F1)	67.8	9.0×10^{4}	0.91	66.1	2.9×10^{4}	0.91
Second-order (F2)	76.5	1.5×10^{6}	0.93	125.6	8.6×10^{11}	0.81
Third-order (F3)	86	3.2×10^{7}	0.93	202.3	2.3×10^{21}	0.75

linkages would be destroyed. The destruction of covalent linkages would greatly accelerate the hydrolysis rate of RS-A in subcritical water, which was opposite to the results shown in Fig. 6a. The hydrolysis of RS-A in the geometrical contraction and the reaction-order models were controlled by R2 and F1 kinetic models, respectively, in all sections; results ascribed to their relatively lower activation energy values. The average activation energies were 205.8, 60.5 and 104.7 kJ mol^{-1} in section I, section II and section III, respectively. The pre-exponential factors of RS-A were in the range of 3.2×10^{18}-8.9×10^{19} min^{-1}, 2.5×10^{1}-1.7×10^{4} min^{-1} and 6.5×10^{0}-4.9×10^{18} min^{-1} in section I, section II and section III, respectively. In contrast, all the kinetic models could be applied to express the hydrolysis kinetics of RS-S in subcritical water (Table 3). Kinetic models of D1 in diffusion models, R2 in geometrical contraction models and F1 in reaction-order models controlled the hydrolysis mechanism of RS-S in both section I and section II. The RS-S showed similar average activation energies in section I (98.8 kJ mol^{-1}) and section II (94.8 kJ mol^{-1}), which was due to the conversion of large amount of cellulose to soluble matters as aforementioned. The pre-exponential factors in section I and section II were calculated to be in the range of 1.2×10^{4}-2.8×10^{12} min^{-1} and 3.4×10^{1}-2.3×10^{21} min^{-1}, respectively.

Compared with the average activation energies of RS, RS-A and RS-S in section I and section II, RS-A and RS-S presented the highest average activation energies in section I and section II, respectively. The higher average activation energy of RS-A might be due to the conversion of amorphous cellulose to soluble matters during pretreatment. The remained cellulose in RS-A were mainly crystalline cellulose, which needed high activation energy to trigger the hydrolysis reaction. In addition, the activation energy of RS-A needed to initiate the hydrolysis reaction in section I was similar to that of microcrystalline cellulose with the value of 226.5 kJ mol^{-1} [36]. The higher average activation energy of RS-S in section II could be ascribed to the high content of lignin remained after pretreatment of RS. Considering all of the experimental and analytical results described

above, it was considered that H_2SO_4 was the most efficient acid to assist ball milling for RS pretreatment, which could be effectively hydrolyzed to value-added chemicals in subcritical water.

Conclusions

Ball milling of RS impregnated with various acids were carried out in the present study. Physicochemical analysis as well as subcritical water hydrolysis was carried out to test the impact of acid species on ball milling treatment of RS. H_2SO_4 was found to be the most active towards destroying hydrogen and glycosidic bonds in RS, because of its relative higher strength and lower volatile. The RS-S showed the highest water solubility, and the lowest crystallinity index and thermal stability among all the samples. The holocellulose-lignin chemical linkages in RS were effectively cleaved after H_2SO_4 impregnation and ball milling treatment, resulting in the increased solid residue yield at the reaction temperature higher than 205 °C. Hydrogen and glycosidic bonds destruction as well as chemical linkages cleavage made RS-S easier to react with subcritical water, leading to the lower activation energy required to initiate the hydrolysis reaction compared with those of RS and RS-A.

Supplementary Information The online version contains supplementary material available at https://doi.org/10.1007/s12649-024-02493-5.

Acknowledgements Financial support from Huzhou Nature Science Foundation (2022YZ25) was acknowledged.

Authors Contribution Investigation, paper writing; F.Y.: Sample preparation, paper writing, supervision; testing and analysis, format and data processing; S.W.: Conception, Supervision, Project management; L.C.: Project supervision, conception.

Funding Prof. WeiYang, Huzhou Nature Science Foundation (2022YZ25).

Data Availability Data will be made available on request.

Declarations

Competing Interests The authors declare that they have no competing interests.

References

1. Qu, T.J., Zhang, X.M., Gu, X.W., Han, L.J., Ji, G.Y., Chen, X.L., Xiao, W.H.: Ball milling for biomass fractionation and pretreatment with aqueous hydroxide solutions. ACS Sustain. Chem. Eng. **5**, 7733–7742 (2017). https://doi.org/10.1021/acssuschemeng.7b01186
2. Okolie, J.A., Nanda, S., Dalai, A.K., Berruti, F., Kozinski, J.A.: A review on subcritical and supercritical water gasification of biogenic, polymeric and petroleum wastes to hydrogen-rich synthesis gas. Renew. Sust Energ. Rev. **119**, 109546 (2020). https://doi.org/10.1016/j.rser.2019.109546
3. Zhang, J.X., Wen, C.T., Zhang, H.H., Duan, Y.Q., Ma, H.L.: Recent advances in the extraction of bioactive compounds with subcritical water: A review. Food Res. Int. **95**, 183–195 (2020). https://doi.org/10.1016/j.tifs.2019.11.018
4. Mattonai, M., Nardella, F., Zaccaroni, L., Ribechini, E.: Effects of milling and UV pretreatment on the pyrolytic behavior and thermal stability of softwood and hardwood. Energy Fuels. **35**, 11353–11365 (2021). https://doi.org/10.1021/acs.energyfuels.1c01048
5. Yang, W., Ma, Y.L., Zhang, X., Yang, F., Zhang, D., Wu, S.J., Peng, H.H., Chen, Z.Z., Che, L.: Effect of acid-associated mechanical pretreatment on the hydrolysis behavior of pine sawdust in subcritical water. Chin. J. Chem. Eng. **58**, 195–204 (2023). https://doi.org/10.1016/j.cjche.2022.11.010
6. Akhtar, N., Gupta, K., Geyal, D., Goyal, A.: Recent advances in pretreatment technologies for efficient hydrolysis of lignocellulosic biomass. Environ. Prog Sustain. **35**, 489–511 (2016). https://doi.org/10.1002/ep.12257
7. Kumar, B., Bhardwaj, N., Agrawal, K., Chaturvedi, V., Verma, P.: Current perspective on pretreatment technologies using lignocellulosic biomass: An emerging biorefinery concept. Fuel Process. Technol. **199**, 106244 (2020). https://doi.org/10.1016/j.fuproc.2019.106244
8. Sun, S.N., Sun, S.L., Cao, X.F., Sun, R.C.: The role of pretreatment in improving the enzymatic hydrolysis of lignocellulosic materials. Bioresour Technol. **199**, 49–58 (2016). https://doi.org/10.1016/j.biortech.2015.08.061
9. Pang, J.F., Zheng, M.Y., Li, X.S., Sebastain, J., Jiang, Y., Zhao, Y., Wang, A.Q., Zhang, T.: Unlock the compact structure of lignocellulosic biomass by mild ball milling for ethylene glycol production. ACS Sustain. Chem. Eng. **7**, 679–687 (2019). https://doi.org/10.1021/acssuschemeng.8b04262
10. Zhang, W., Zhang, X., Liang, M., Lu, C.: Mechanochemical preparation of surface-acetylated cellulose powder to enhance mechanical properties of cellulose-filler-reinforced NR vulcanizates. Compos. Sci. Technol. **68**, 2479–2484 (2008). https://doi.org/10.1016/j.compscitech.2008.05.005
11. Dell'Omo, P.P., Spena, V.A.: Mechanical pretreatment of lignocellulosic biomass to improve biogas production: Comparison of results for giant reed and wheat straw. Energy. **203**, 117798 (2020). https://doi.org/10.1016/j.energy.2020.117798
12. Nuruddin, M., Hosur, M., Uddin, M.J., Baah, D., Jeelani, S.: A novel approach for extracting cellulose nanofibers from lignocellulosic biomass by ball milling combined with chemical treatment. J. Appl. Polym. Sci. **9**, 42990 (2016). https://doi.org/10.1002/app.42990
13. Liu, X.L., Dong, C.Y., Leu, S.Y., Fang, Z., Miao, Z.D.: Efficient saccharification of wheat straw pretreated by solid particle-assisted ball milling with waste washing liquor recycling. Bioresour Technol. **347**, 126721 (2022). https://doi.org/10.1016/j.biortech.2022.126721
14. Sitotaw, Y.W., Habtu, N.G., Gebreyohannes, A.Y., Nunes, S.P., Gerven, T.V.: Ball milling as an important pretreatment technique in lignocellulose biorefneries: A review. Biomass Convers. Biorefin. **9**, 8232–8237 (2021). https://doi.org/10.1007/s13399-021-01800-7
15. Shen, F., Xiong, X.N., Fu, J.Y., Yang, J.R., Qiu, M., Qi, X.H., Tsang, D.C.W.: Recent advances in mechanochemical production of chemicals and carbon materials from sustainable biomass resources. Renew. Sust Energ. Rev. **130**, 109944 (2020). https://doi.org/10.1016/j.rser.2020.109944

16. Dornath, P., Cho, H.J., Paulsen, A., Dauenhauer, P., Fan, W.: Efficient mechano-catalytic depolymerization of crystalline cellulose by formation of branched glucan chains. Green. Chem. **17**, 769–775 (2015). https://doi.org/10.1039/C4GC02187H
17. Shrotri, A., Lambert, L.K., Tanksale, A., Beltramini, J.: Mechanical depolymerisation of acidulated cellulose: Understanding the solubility of high molecular weight oligomers. Green. Chem. **15**, 2761–2768 (2013). https://doi.org/10.1039/C3GC40945G
18. Carrasquillo-Flores, R., Kaldstrom, M., Schuth, F., Dumesic, J.A., Rindldi, R.: Mechanocatalytic depolymerization of dry (Ligno)cellulose as an entry process for high-yield production of furfurals. ACS Catal. **3**, 993–997 (2013). https://doi.org/10.1021/cs4001333
19. Zhao, L.L., Chen, X.F., Liu, X.Y., Xu, G.Q., Guo, X.C., Yang, Y.: Highly efficient synthesis of C5/C6 sugar alcohols from bamboo enabled by mechanocatalytic depolymerization. ACS Sustain. Chem. Eng. **9**, 6697–6706 (2021). https://doi.org/10.1021/acssuschemeng.1c00469
20. Hilgert, J., Meine, N., Rinaldi, R., Schuth, F.: Mechanocatalytic depolymerization of cellulose combined with hydrogenolysis as a highly efficient pathway to sugar alcohols. Energy Environ. Sci. **6**, 92–96 (2013). https://doi.org/10.1039/c2ee23057g
21. Yang, Y., Hu, C.W., Abu-Omar, M.M.: Conversion of carbohydrates and lignocellulosic biomass into 5-hydroxymethylfurfural using $AlCl_3{\cdot}6H_2O$ catalyst in a biphasic solvent system. Green. Chem. **14**, 509–513 (2012). https://doi.org/10.1039/C1GC15972K
22. Mandal, A., Chakrabarty, D.: Isolation of nanocellulose from waste sugarcane bagasse (SCB) and its characterization. Carbohydr. Polym. **86**, 1291–1299 (2011). https://doi.org/10.1016/j.carbpol.2011.06.030
23. Zhao, J.K., Yang, Y., Zhang, M., Wang, D.H.: Minimizing water consumption for sugar and lignin recovery via the integration of acid and alkali pretreated biomass and their mixed filtrate without post-washing. Bioresour Technol. **337**, 125389 (2021). https://doi.org/10.1016/j.biortech.2021.125389
24. Liu, H., Chen, X.L., Ji, G.Y., Yu, H.T., Gao, C.F., Han, L.J., Xiao, W.H.: Mechanochemical deconstruction of lignocellulosic cell wall polymers with ball-milling. Bioresour Technol. **286**, 121364–121371 (2019). https://doi.org/10.1016/j.biortech.2019.121364
25. Yao, W.Q., Weng, Y.Y., Catchmark, J.M.: Improved cellulose X-ray diffraction analysis using Fourier series modeling. Cellulose. **27**, 5563–5579 (2020). https://doi.org/10.1007/s10570-020-03177-8
26. Ling, Z., Wang, T., Makarem, M., Cintron, M.S., Cheng, H.N., Kang, X., Bacher, M., Potthast, A., Rosenau, T., King, H., Delhom, C.D., Nam, S., Edwards, J.V., Kim, S.H., Xu, F., French, A.D.: Effects of ball milling on the structure of cotton cellulose. Cellulose. **26**, 305–328 (2019). https://doi.org/10.1007/s10570-018-02230-x
27. Schuth, F., Rinaldi, R., Meine, N., Kaldstrom, M., Hilgert, J., Kaufman Rechulski, F.D.: Mechanocatalytic depolymerization of cellulose and raw biomass and downstream processing of the products. Catal. Tooday. **234**, 24–30 (2014). https://doi.org/10.1016/j.cattod.2014.02.019
28. Xiao, Z.Q., Yang, Q.Q., Xu, X.Y., He, Y.F.: Ball milling promotes saccharification of agricultural biomassby heteropolyacid and enzyme: Unlock the lignin cage for sugars recovery. Biomass Conv Bioref. **12**, 4105–4115 (2022). https://doi.org/10.1007/s13399-020-00950-4
29. Ersan, S., Guclu Ustundag, O., Carle, R., Schweiggert, R.M.: Subcritical water extraction of phenolic and antioxidant constituents from pistachio (Pistacia vera L.) hulls. Food Chem. **253**, 46–54 (2018). https://doi.org/10.1016/j.foodchem.2018.01.116
30. Yang, W., Fang, M.N., Xu, H., Wang, H., Wu, S.J., Zhou, J., Zhu, S.X.: Interactions between holocellulose and lignin during hydrolysis of sawdust in subcritical water. ACS Sustain. Chem. Eng. **7**, 10583–10594 (2019). https://doi.org/10.1021/acssuschemeng.9b01127
31. Fang, Z., Minowa, T., Smith, R.L., Ogi, T., Kozinski, J.A.: Liquefaction and gasification of cellulose with Na_2CO_3 and ni in subcritical water at 350°C. Ind. Eng. Chem. Res. **43**, 2454–2463 (2004). https://doi.org/10.1021/ie034146t
32. Buhler, W., Dinjus, E., Ederer, H.J., Kruse, A., Mas, C.: Ionic reactions and pyrolysis of glycerol as competing reaction pathways in near- and supercritical water. J. Supercrit Fluids. **22**, 37–53 (2002). https://doi.org/10.1016/S0896-8446(01)00105-X
33. Sasaki, M., Adschiri, T., Arai, K.: Kinetics of cellulose conversion at 25 MPa in sub- and supercritical water. AIChE J. **50**, 192–202 (2004). https://doi.org/10.1002/aic.10018
34. Lawoko, M., Henriksson, G., Gellerstedt, G.: Characterisation of lignin-carbohydrate complexes (LCCs) of spruce wood (*Picea abies* L.) isolated with two methods. Holzforschung. **60**, 156–161 (2006). https://doi.org/10.1515/HF.2006.025
35. Zhang, X.L., Yang, W.H., Blasiak, W.: Modeling study of woody biomass: Interactions of cellulose, hemicellulose, and lignin. Energy Fuels. **25**, 4786–4795 (2011). https://doi.org/10.1021/ef201097d
36. Yang, W., Shimanouchi, T., Wu, S.J., Kimura, Y.: Investigation of the degradation kinetic parameters and structure changes of microcrystalline cellulose in subcritical water. Energy Fuels. **28**, 6974–6980 (2014). https://doi.org/10.1021/ef501702q